Properties of Bioriented Nylon 6 Films Related to Film Production Technology

F. Bianchi,[1] S. Cantagallo,[1] G. Consolati,[2] M. Laporta,[1] M. Pegoraro,[1] G. Tieghi,[1] L. Zanderighi[3]

[1]*Department of Industrial Chemistry and Chemical Engineering, Politecnico Milano, Pza Leonardo da Vinci 32-20133, Milano, Italy*
[2]*Istituto Nazionale per la Fisica della Materia, Department of Physics, Politecnico di Milano, Pza Leonardo da Vinci 32-20133, Milano, Italy*
[3]*Department of Physical Chemistry and Electrochemistry, University of Milano, Via Golgi 19-20133, Milano, Italy*

Received 18 April 2000; accepted 15 October 2001

ABSTRACT: Four production steps, extrusion, blowing, stabilization, and finishing, are involved in the manufacture of biorented nylon 6 films. The films obtained after each step were studied by wide-angle diffraction X-rays, IR analysis, and density measurements. Orientation in the amorphous phase was evaluated by thermal retraction. Free volume was investigated by positron annihilation spectroscopy. Mechanical properties were tested by tensile tests, and permeability was tested with isopiestic permeameters. Quenching, after extrusion, generated an unstable γ crystalline phase and an amorphous phase. Blowing transformed the unstable γ phase into the thermodynamically stable α phase and increased the chain orientation; stabilization increased α phase crystals, favored hydrogen bond formation and, therefore, the mechanical properties, leaving unchanged the chain orientation; the final treatment increased the mechanical properties. The film permeabilities to O_2, N_2, and CO_2 were practically unchanged after each production step; this result may be explained by considering that the nanoholes, present in the films and responsible for the diffusion inside the polymer, maintained practically constant their radius, whereas their number concentration decreased slowly after thermomechanical treatments. © 2002 Wiley Periodicals, Inc. J Appl Polym Sci 86: 559–571, 2002

Key words: nylon 6; bioriented films; production of films

INTRODUCTION

Food packaging film is a major area of application for nylon 6 homopolymers. Films are used alone or as part of multilayered structures. Nylon 6 films provide flavor and aroma barriers and, under dry conditions, are moderately good oxygen barriers.

Thermomechanical treatments of nylon 6 films induce remarkable variations of their structural microphase composition with significant effects on mechanical and IR absorption spectra. To our knowledge, no exhaustive effort has been undertaken until now regarding the evolution of the structure, morphology, and mechanical and transport properties during the various technological steps in the production of bioriented nylon 6 films. This was, therefore, the aim of this study.

In the production process of the bioriented nylon 6[1] that we studied, four subsequent steps could be recognized (Fig. 1). The first one involved extrusion through an annular die followed by quenching in water. After drying, we got a tubular film (TF) with a wall thickness of about 140 μm. The second step consisted of a blowing operation with air, preceded by a radiant heating that raised the temperature of the TF (with diameter D_0) just above the glass-transition temperature (about 325 K). In these conditions, the compliance was sufficiently high to allow a plastic deformation. The internal air pressure gave rise to a transversal strain so as to increase the diameter of the TF to a value $D_1 = \lambda_2 D_0 \cong 3D_0$. At the same time, the film underwent a longitudinal elongation ratio $\lambda_1 = v/v_0 = 3$ due to the different rotation speeds of the collecting rolls (v) and the feeding rolls (v_0). The freezing line, by a proper cooling with air, was located at the position where the tube diameter had reached the value D_1 (Fig. 1). During the blowing, the film thickness was strongly reduced, and the original organization of crystallites in the TF was deeply modified due to the high elongation ratios (λ_1 and λ_2), which were applied, and brought the material beyond its yield point: this destroyed the original morphology and structure. Consequently, a bioriented state of the molecules and crystalline lamellas was reached, which was frozen in during the cooling of the film from the blowing temperature to room temperature. The TF was flattened and cut longitudinally at the edges in a continuos way; at this stage, the film was called bioriented *blown film* (BF).

The third step stabilized the size of the BF. By heating the BF, we prevented the natural retraction, which

Correspondence to: M. Pegoraro (mario.pegoraro@pol.mi.it).

Journal of Applied Polymer Science, Vol. 86, 559–571 (2002)

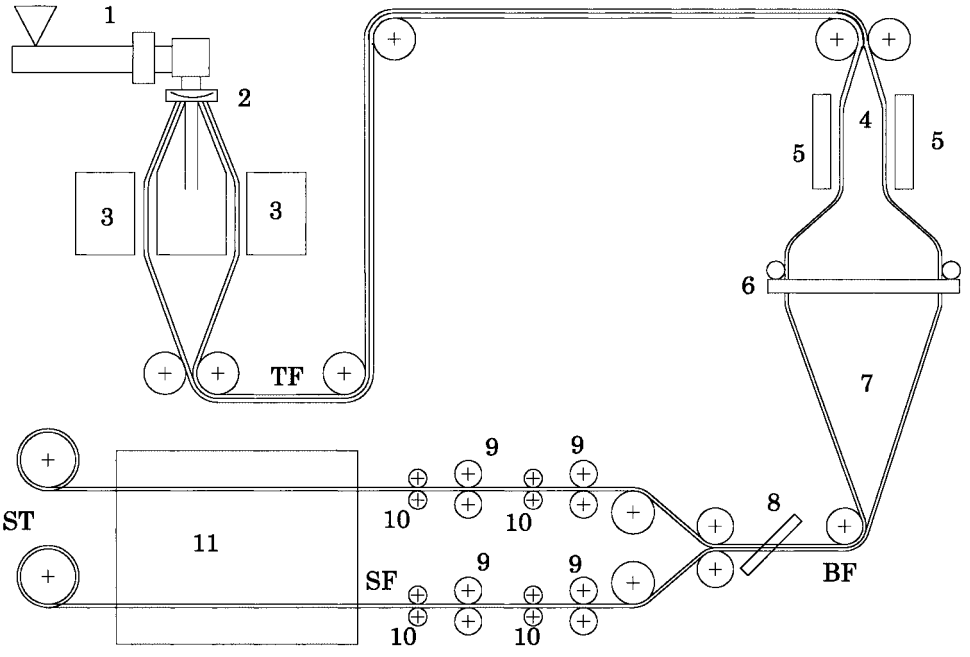

Figure 1 Scheme of nylon film manufacture.

should occur in the absence of mechanical constraints, by operating with four special rolls, each one endowed at the contour with grips that pressed down the film edges so contrasting its transversal shrinkage due to entropic retraction forces. We also prevented the longitudinal shrinkage by imposing increasing rotating speeds to the rolls put in series. In the former roll couple, the first roll, kept at 405 K, was followed by the second one cooled down. In the latter couple, the first roll was heated up to 425 K, and the second one was cooled down.

In the temperature range of the hot rolls (405–425 K), the crystallization rate of the nylon 6 film was at its maximum value.[2] In the same temperature range, the stress relaxation time in the amorphous regions was short,[3] but the chains could not lose their orientation because of the mechanical constraints. In this way, stress relaxation took place, and orientation was preserved. Both of these phenomena increased crystallinity. The two couples of rolls allowed a fine-tuning of the operating parameters related to the quality of the final product. At the end of this stage the film was called *stabilized film* (SF). In the last step (the finishing operation), the SF was treated in an air oven where the stabilization procedure was completed by a further reduction of the residual internal stresses. The obtained film was called the *final film* (ST).

EXPERIMENTAL

X-ray diffraction patterns were recorded with a Philips (Eindhoven, Holland) PW1050-1710 diffractometer with CuKα radiation.

Density (ρ) was measured on dry samples with the Archimede's principle (ASTM D 792 91) in cyclohexane (ρ = 0.77855 g/cm^3).

For positron annihilation spectroscopy (PAS) measurements, the positron source consisted of ^{22}Na deposited between two Kapton foils (DuPont; 1.08 mg/cm^2). We prepared the sample by overlapping a convenient number of nylon films; the total thickness of the material was sufficient to stop all the injected positrons. Positron spectra were collected through a conventional fast–fast coincidence setup. The source–sample assembly was inserted into a glass container connected to a standard vacuum system (5×10^{-5} mbar). Each spectrum collected about 10 Mcounts. Deconvolutions were carried out through the computer code LT,[4] with a suitable correction for positrons annihilated in the Kapton.

Concerning the thermoretraction measurements, film samples (length L_0 = 120 mm in the draw direction, width = 12 mm) were placed horizontally on a paper sheet, covered by talcum powder to reduce friction, and then put in an oven at the chosen temperature (353, 373, 403, 433, or 473K) for 3 h. After being cooled at room temperature for 1 h, the length (L_f) of the films were measured, and the retraction index $RI = (L_f - L_0)/L_0$ was calculated.

Tensile properties of the films [yield stress (σ_y), break strength, and corresponding strains] were measured with an Instron (England) 4302 dynamometer according to ASTMD 638 in a thermostatic room at 296 K and 50% relative humidity. The tensile elastic modulus was also measured with a proper strain gauge. The elongation rate was 10 mm/min.

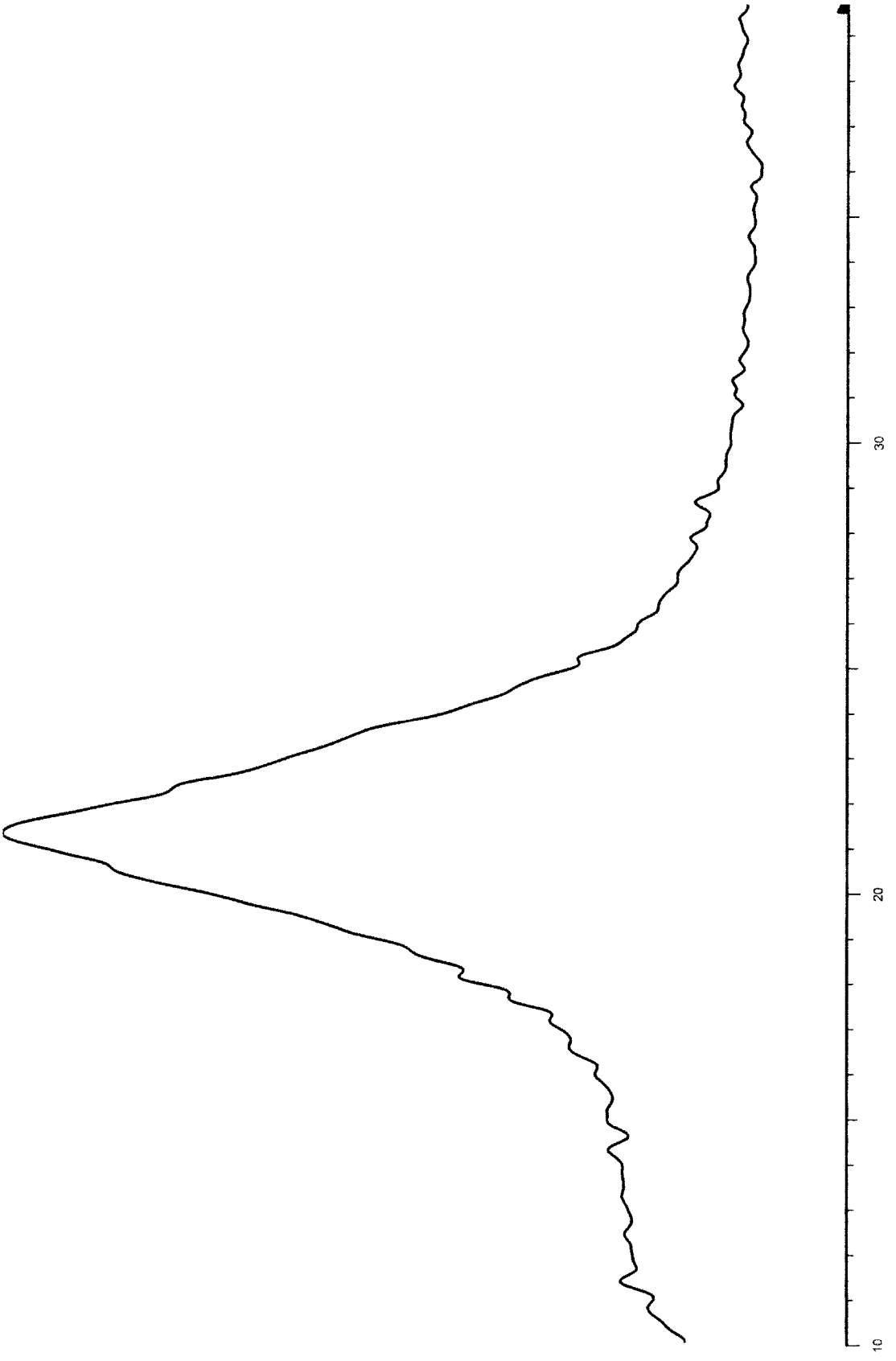

Figure 2 X-ray diffraction of TF.

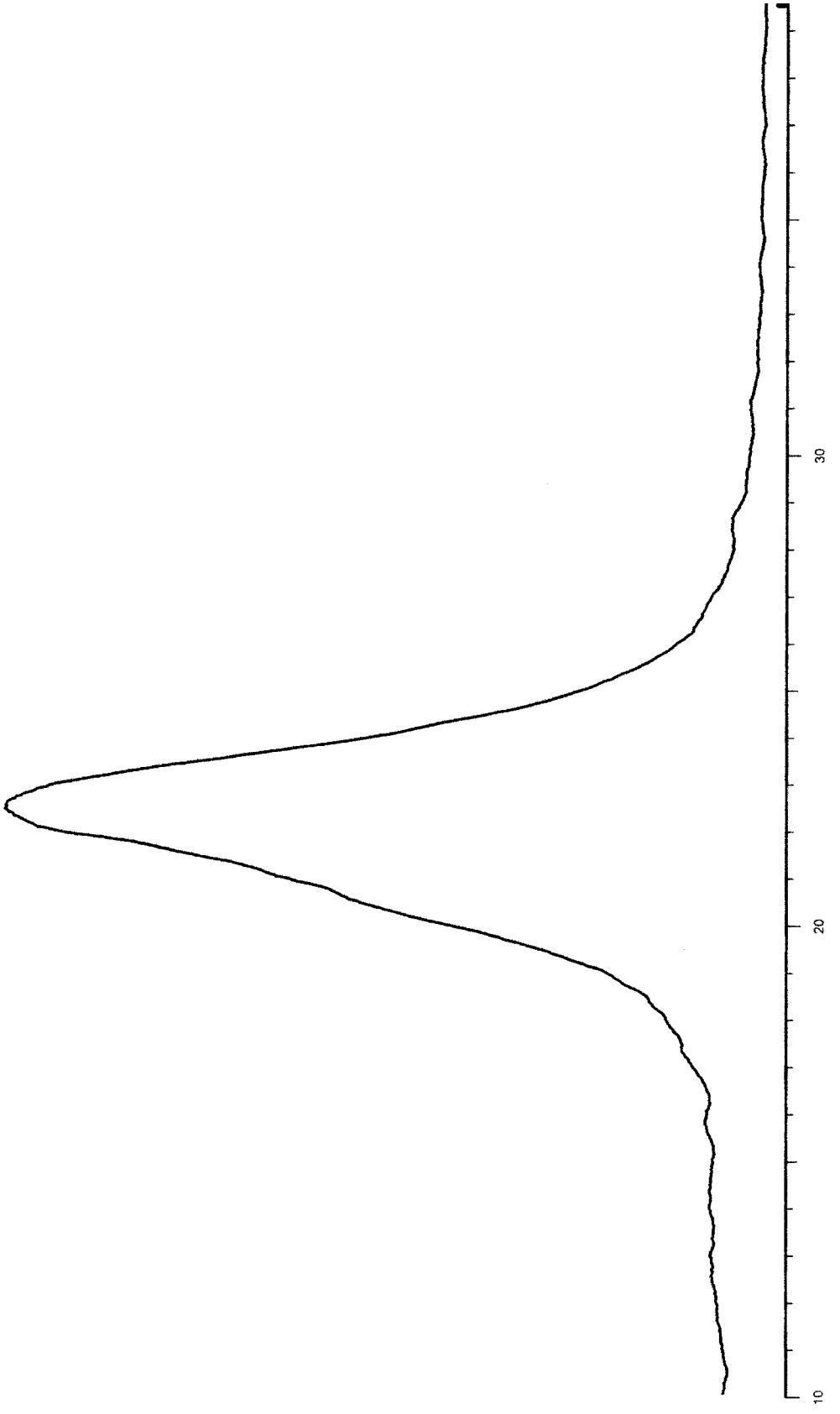

Figure 3 X-ray diffraction of BF.

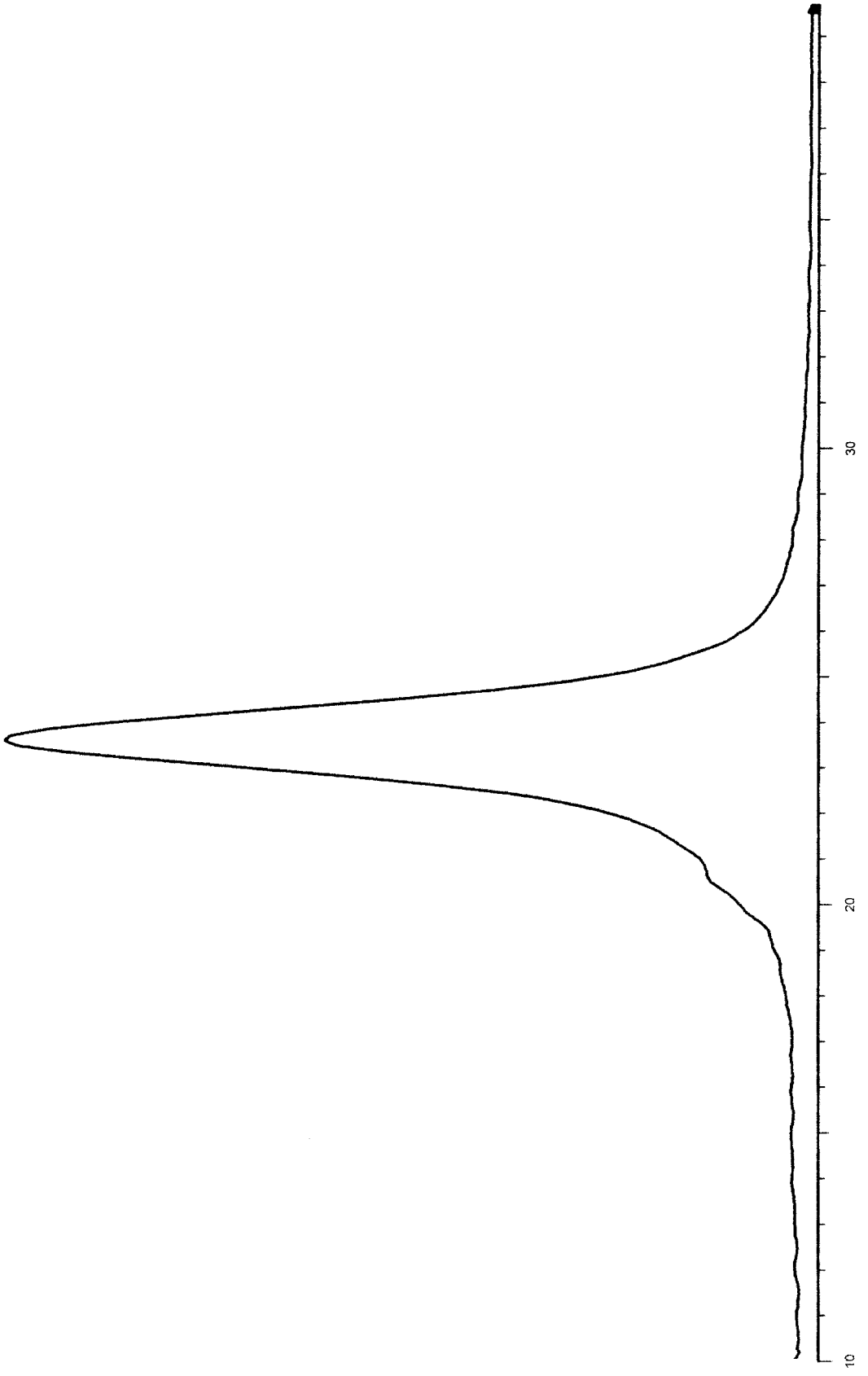

Figure 4 X-ray diffraction of SF.

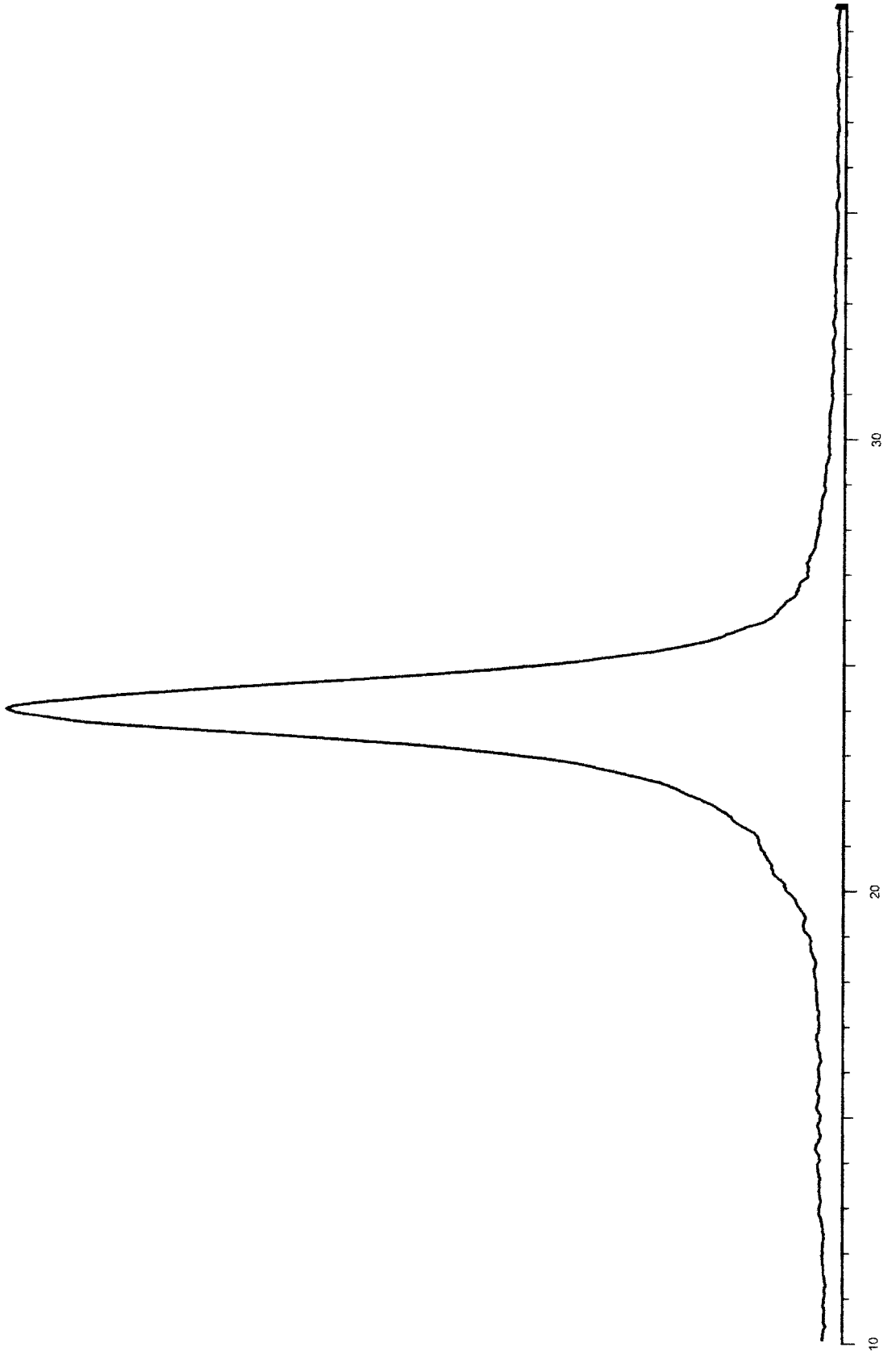

Figure 5 X-ray diffraction of ST.

Permeability tests were performed with an isopiestic apparatus in which the permeated gas was collected in a He stream and analyzed by gas chromatography. The permeability was determined from the accumulation rate of the permeated gas.[5]

RESULTS AND DISCUSSION

Structural characterization of the films

Mechanical and thermal treatments produced remarkable structural modifications of the TF, as shown by the X-ray diffraction patterns (Figs. 2–5) of the films at the different processing stages.

The TF (Fig. 2) showed a rather wide peak, with a maximum near 21.3° 2θ, which is typical of the nylon 6 γ phase.

In the BF (Fig. 3), the peak width appeared slightly narrower and shifted toward higher angles, with a double maximum at 22.2–22.8° 2θ and a shoulder around 20.5° 2θ. Because the stable monoclinic α phase is characterized by two peaks at 20.2° 2θ (200 reflection) and 24.0° 2θ (202 and 002 reflections), it may be supposed that in the BF, the α and γ phases were contemporary present. However, Huisman and Heuvel[6,7] showed that if the α phase is highly defective, the positions of the 202 and 002 diffraction peaks can be considerably displaced toward lower angles. Thus, the pattern of the BF could be attributed to a defective α phase obtained from the transformation of the γ phase, favored by the effect of mechanical orientation due to the blowing process (the low intensity of the 200 reflection peak is a consequence of orientation).

In the diffraction patterns of the SF (Fig 4) and ST (Fig 5), the peaks corresponding to the 202 and 002 reflections of the α phase occurred at 23.5 and 23.9° 2θ, respectively. This, together with the increase of intensity and a noticeable progressive reduction of the peak width, indicated qualitatively that the thermal treatments produced an increase of the crystal size and a decrease in the defects, leading on the whole, to a higher degree of crystallinity (χ).

Unfortunately, meaningful quantitative values of χ could not be obtained from the X-ray diffraction patterns because a completely amorphous sample film of nylon 6 was not available to get the amorphous phase reference pattern.

On the contrary, χ could be calculated from ρ measurements by the relation

$$\chi = \frac{V_a - V}{V_a - V_c} = \frac{\rho_c}{\rho} \cdot \frac{\rho - \rho_a}{\rho_c - \rho_a} \qquad (1)$$

where V, V_a, and V_c are the specific volumes and ρ, ρ_a, and ρ_c are the densities of the films, respectively, of a completely amorphous and a completely crystalline sample. The measured values of the densities of the films are reported in Table I.

TABLE I
ρ and χ for Films at the Different Steps

Film	ρ (g/cm^3)	χ (%)
TF	1.127	41
BF	1.147	48
SF	1.152	51
ST	1.153	52

The ρ values of the completely crystalline α phase (1.225 g/cm^3) and of the completely amorphous (1.084 g/cm^3) nylon 6 were taken from Roldan and Kaufman.[8] These values were used to calculate χ of the BF, SF, and ST; the ρ of the completely crystalline γ phase (1.194 g/cm^3) present in the TFs, was calculated from the unit cell parameters given by Arimoto et al.[9] The values of χ obtained from eq. (1) are reported in Table I; these values were in full agreement with the qualitative structural indications drawn from the X-ray diffraction pattern.

IR spectroscopy

In Table II, according to literature,[10–13] twelve absorbance wavenumbers attributed to different atomic or group vibrations of nylon 6 are shown. However, we could not always find clear attributions of each wavenumber to the nylon structural phases in which the vibrations may occur. Therefore, we used the following empirical procedure to study the structural modifications induced by the technological steps: (1) the absorbance of films corresponding to the four steps were compared; and (2) with the aim of eliminating any possible experimental noise, one absorbance wavenumber was chosen as a reference (internal standard) and the absorbance of each sample were normalized with respect to this one. The reference absorbance was chosen analyzing the adsorbance of the twelve wavenumbers and considering that one which shows the minimum variation.

In Table III, the absorbance data of the twelve IR absorption bands of the four samples are reported. Because the TF had a large thickness, the absorbance for wavenumbers over 1100 cm^{-1} were practically 100%, so no transmittance peak was recorded in that region.

The statistical analysis of the absorbance data (Table III) of the BF, SF, and ST, which had comparable thicknesses, indicated that one band may be considered to have a constant adsorbance. This band occurs at 1463 cm^{-1}; the variation on the mean value over all the samples was lower than 5%. Therefore, for each sample, the absorbance at 1463 cm^{-1} was used as internal standard for IR spectra analysis. The standardized values ($A_{\nu i}/A_{1463}$) are reported in Figure 6

TABLE II
Attribution of Wavelengths to Different Groups in Nylon 6 of Different Phases

Absorption peak (cm^{-1})	Resonant group	Phase	Reference
1475	CH_2 (b) vic. NH	α	10, 11
1463	CH_2 (b)	γ + amorphous	11
1436	CH_2	γ + amorphous	11
1415	CH_2 (b) ad. CO	α	11
1277	CH_2 (w)	amorphous	11, 12
1200		α	11
1170		amorphous (+ γ)	11
1119	C—C (s)	amorphous	11, 12
1027	CO—NH in plane	amorphous	10, 12
980		amorphous	11, 12
959	C—CO (s)	α	11
928	C—CO (s)	α	11

s, stretching; b, bending; w, wagging; vic., vicinal; ad., adjacent.

for each of the films: BF, SF, and ST. The main differences among the samples in the twelve absorbances were evident. The values for TF were omitted.

In Figure 7, each standardized absorbance is reported as a function of the sample type (BF, SF, or ST). All bands attributable to the α phase (1475, 1415, 1200, 959, and 928 cm^{-1}) evidenced a clear increase from BF to ST; the other bands, assigned to the amorphous phase or to the γ phase showed a decrease (1436, 1277, 1179, and 1027 cm^{-1}) with the exception of the absorption peak at (980) that practically did not change. Two peaks seemed of practical interest: the 1277 cm^{-1} peak typical of the amorphous phase, which evidenced a strong change from BF to SF and only a small change from SF to ST; the other was the peak at 1200 cm^{-1}, typical of the α phase, which continuously increased from BF to ST. These two bands may be used for a continuous process control of nylon film production.

PAS

The positron annihilation spectra were analyzed into three components. Two of them were assumed to decay exponentially, with a single lifetime (τ; "discrete" components); on the other hand, the third component was supposed to be a distribution of τs. The first two components took into account annihilations of positrons not forming positronium (Ps) and annihilated from various states (in the bulk of the structure, in the free volume, or trapped in defects in the crystalline zones), as well as annihilations of para-Ps. This last component could not be distinguished from annihilations of positrons in the bulk because of the resolution of the apparatus. The most interesting component was the third one, which represented ortho-Ps decays in the holes forming the free volume of the polymer. The values of the parameters characterizing this distribution of τs (centroid, standard deviation, and relative intensity) are shown in Table IV for the different examined structures. The average τ can be correlated to the dimensions of the cavity through a simple quantum–mechanical model:[14,15] the hole is approximated by a spherical well having a radius (R_0), to confine Ps with a potential that becomes infinite on the walls. This last in the triplet sublevel is annihilated in most cases by an external electron belonging to one of the molecular orbitals that form the surface layer of the hole (this it is known as the *pick-off process*[16]). A thickness (ΔR) is introduced to take this layer into account so that the effective radius of the cavity is $R = R_0 - \Delta R$. The correlation between the ortho-Ps τ [τ (ns)] and the radius R (Å) was given by the following equation:

$$\tau^{-1} = 2\left[1 - \frac{R}{R_0} + \frac{1}{2\pi}\sin\left(2\pi\frac{R}{R_0}\right)\right] \qquad (2)$$

where $\Delta R = 1.66$ Å, as obtained through a fitting of annihilation data in porous structures having known

TABLE III
Relative Absorption Intensities at the Various Wavenumbers (cm^{-1}) for the Four Films

Sample	1475	1415	1463	1436	1200	1277	1170	1119	1027	980	959	928
TF	0	0	0	0	0	0	0	0.0170	0.0070	0.0115	0.0088	0.0067
BF	0.0629	0.0589	0.0770	0.0647	0.0509	0.0577	0.0442	0.0227	0.0156	0.0134	0.0121	0.0121
SF	0.0760	0.0748	0.0863	0.0610	0.0705	0.0183	0.0404	0.0225	0.0158	0.0158	0.0177	0.0162
ST	0.0753	0.0731	0.0823	0.0536	0.070	0.0142	0.0349	0.0230	0.0123	0.0138	0.0181	0.0186

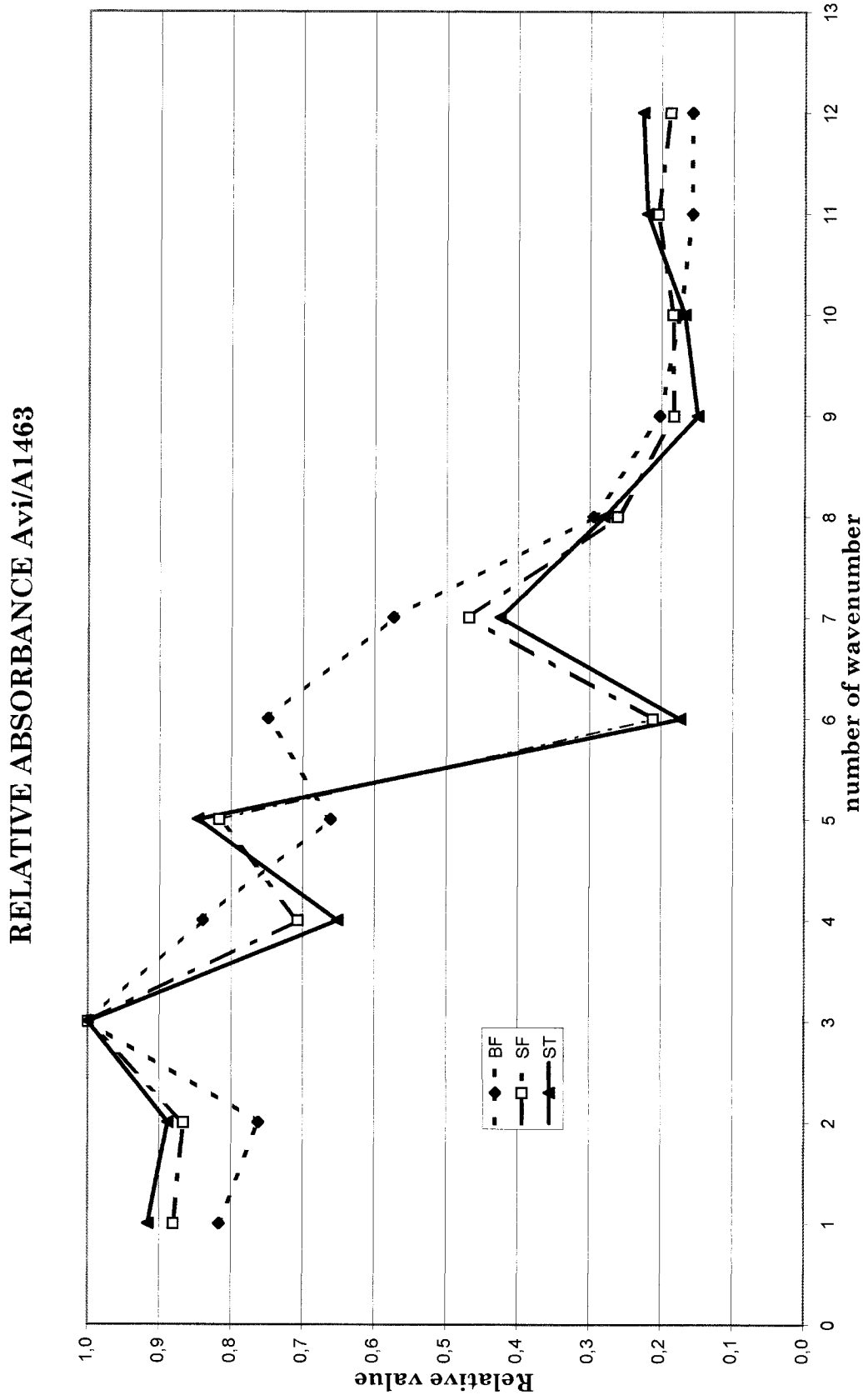

Figure 6 Standardized ratios $A_{\nu i}/A_{1463}$ versus wavenumber. (See Table III for wavenumbers.)

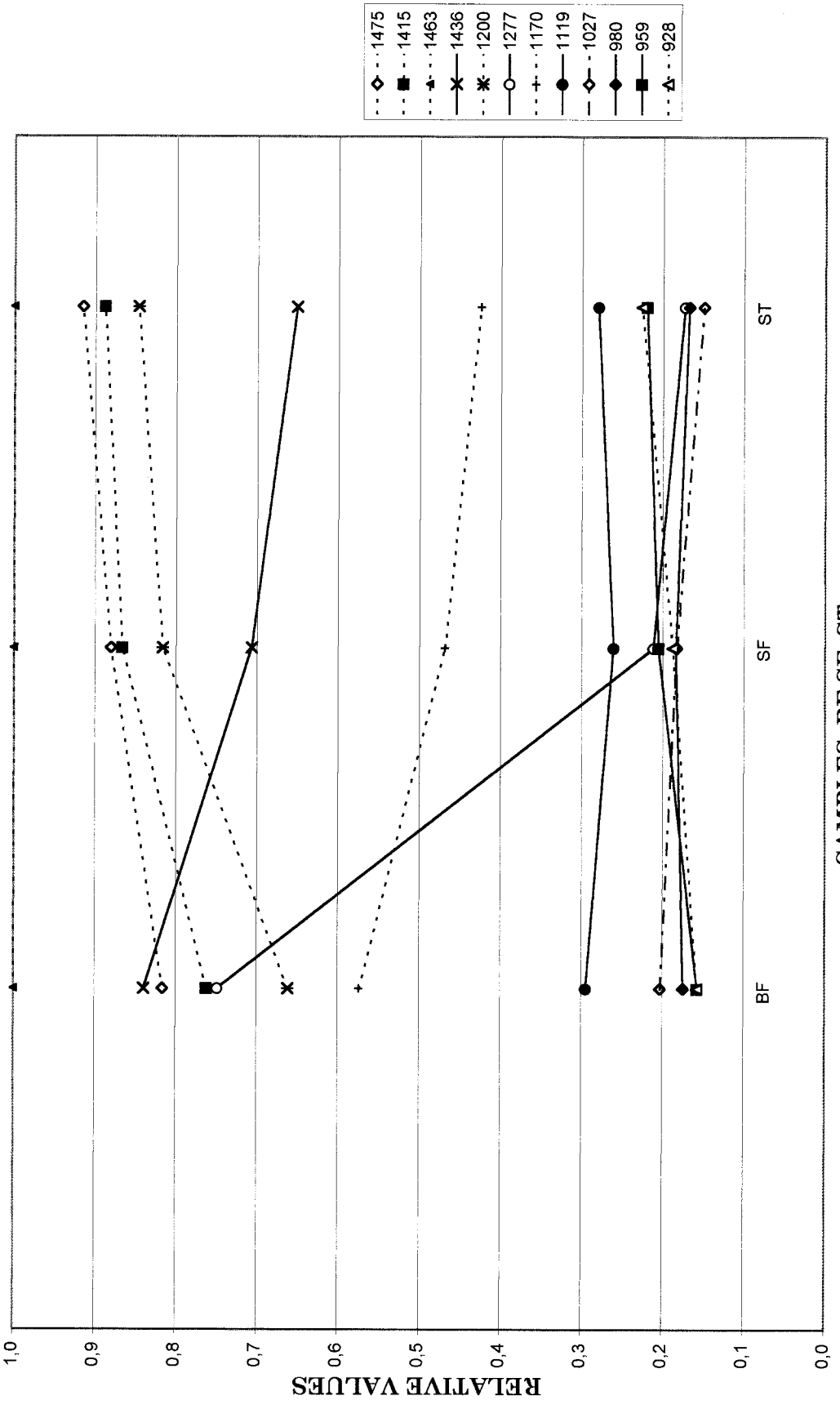

Figure 7 Comparative evaluation of the relative absorbances of the various type of films.

TABLE IV
Hole Radius and Volume in Nylon 6 During Transformation

	Lifetime distribution				Volume (Å^3)	
Nylon 6	Centroid τ (ns)	Standard deviation	Intensity	Radius (Å)	Centroid	Standard deviation
TF	1.56 ± 0.05	0.24 ± 0.02	28.0 ± 0.8	2.39 ± 0.06	55.2 ± 0.3	19 ± 2
BF	1.58 ± 0.05	0.22 ± 0.02	26.5 ± 0.7	2.42 ± 0.06	57.1 ± 0.3	18 ± 2
SF	1.53 ± 0.05	0.26 ± 0.02	27.6 ± 0.8	2.36 ± 0.06	52.4 ± 0.3	20 ± 2
ST	1.54 ± 0.05	0.21 ± 0.02	24.8 ± 0.6	2.38 ± 0.06	54.8 ± 0.3	17 ± 2

dimensions.[17] Our data can be interpreted in terms of average radii of holes; as seen in an inspection of Table IV, such radii did not change significantly, showing a mean value around 2.4 Å.

Obviously, our data should be interpreted as approximate because the holes were not spherical, as assumed in our model, but were irregular.

If we accept the existence of a distribution of the radii of the holes, it is reasonable to correlate it to the distribution of ortho-Ps τs; analysis of the annihilation time spectrum gave also the second moment (standard deviation) of such a distribution, shown in the third column of Table IV. With a suitable transformation;[18] we obtained the second moment of the distribution of the volumes of the holes, which is shown in the last column of the table.

Also in this case, we did not observe large differences; however, the trend was toward a decrease of the standard deviation. We conclude that the thermal treatments did not have a strong influence on the volumes of the nanoholes, rather they tended to homogenize their distribution function. Relative intensity analysis of the ortho-Ps component revealed that it decreased on passing from the TF to the stretched ST. The intensity parameter is related to the formation probability of Ps, and it changes monotonously with the concentration of the holes by an assumption that Ps is formed in the free volume of the polymer.[19] The total free volume, as a whole, decreases because the mean volume of cavities does not change in the limits of the experimental error, whereas the number of cavity decreases. Such a result is consistent with the behavior of the ρ, which increases during the various phases of polymer manufacturing; it corresponds to an increase of χ in the structure and, therefore, to a shrinking of the amorphous zones. Although we cannot give a quantitative relationship between crystallinity and Ps intensity due to the uncertainties associated to this parameter, it is nevertheless interesting to observe that their trends are in agreement each other and allow us to give a consistent interpretation of the variations of the free volume.

Thermoretraction

Table V shows the retraction index (RI %) at 423 K of the films at the different process steps, both in the longitudinal and in the transversal directions. This index is an indirect measure of the orientation of the polymer chains in the amorphous phase. In fact, the considered retraction temperature is well below the melting temperature (492.3 K) so that the rigid lamellas are involved in the retraction mechanism only for the viscous resistance they oppose to the recoiling of the amorphous chains. Different retractions existed after any step of the process, and the maximum increment of orientation was reached after the blowing step. The small differences of index RI in the transversal and longitudinal directions could have been related technologically to the fluctuations of pressure and rotating speed of the rolls of the plant. The high increase of the film area ($\lambda_1\lambda_2 \cong 9$) during the blowing was accompanied by a strong reduction of the thickness (Table V).

Retraction after the blowing step was much higher than after the stabilization step and was almost eliminated in the final step. This shows that a high chain orientation was present after blowing in the amorphous state. During the stabilization step, these chains could easily crystallize because they could not coil up due to the local mechanical constraints and because the temperature was kept at the level at which the crystallization rate was maximum (403–413°K)

Although the film area could not be reduced, during stabilization thickness reduction was not prevented (Table V), and in fact, a decrease of about 30% was observed. It was not easy to foresee exactly the evolution of morphology during the stabilization step because on the one hand, the bioriented amorphous parts of chains should have been able to crystallize, to recoil, or to slip; on the other hand, they were connected with the rigid lamellas, which were oriented

TABLE V
Thickness of the Films at the Different Steps of the Process and Their Retraction Index at 423 K in the Longitudinal and Transversal Directions

Type of film	Thickness (μm)	Retraction index ($-\Delta L/L$) %	
		Longitudinal	Transversal
TF	137.4 ± 0.9	1.75	1.25
BF	18.0 ± 0.2	21.3	18.8
SF	13.3 ± 0.4	2.9	2.9
ST	15.5 ± 0.5	0.75	0.75

TABLE VI
Mechanical Properties at Different Steps of the Process Measured Both in Longitudinal (L) and Transverse (T) Directions

	TF		BF		SF		ST	
Type of film	L	T	L	T	L	T	L	T
Elastic modulus (MPa)	19.5 ± 0.6	19 ± 2	132 ± 13	126 ± 20	233 ± 20	258 ± 21	320 ± 28	350 ± 28
σ_y (MPa)	27.8 ± 0.5	28.8 ± 0.5	31 ± 1	30 ± 1	38.5 ± 0.3	32 ± 0.3	44 ± 1	37 ± 1
ε_y (%)	11.2	13.6	5.1	5.2	5.6	5.2	3.9	3.7
Tensile stress (MPa)	36.8	35.6	34.5	35.6	52.4	50.3	61.3	57.5
Strain at break (%)	180	184	32	33	21	18	18	16

during the blowing step. Lamellas may hinder, at least partly, the motions of the amorphous chains but could be moved themselves in the highly viscous system to reach even higher orientations compatible with a higher ρ. PAS analysis was not able to show any free volume variation that can explain in the amorphous phase the ρ increase and the thermoretraction result.

Mechanical properties

Table VI shows the values of the elastic modulus, σ_y and yield strain (ϵ_y), and stress and strain at break of the films at the various process steps, both in the longitudinal and transverse directions.

For all properties, the differences in the longitudinal and transverse directions were generally small, both for the unoriented TF and the bioriented ones. What did change at the various process steps was mainly the value of the property. In particular, a large increment of the elastic modulus was obtained in the blowing step, which mainly produced the biorientation and also an increase of crystallinity. A further increase of the elastic modulus was produced by the stabilization step due to the crystallinity increase. A remarkable increase of the elastic modulus could be observed after the thermal treatment of the finishing step. This increase could not be attributed to a further crystallization (see Table I) but, probably, to a different organization of the remaining amorphous regions, which can retract in the absence of constraints and give rise to a thickness increase (Table V). A similar (increasing) behavior was shown by σ_y, whereas ϵ_y regularly decreased with the process steps. The contemporary increment of σ_y and decrement of ϵ_y were in agreement with the increase of elastic modulus. Finally, the film strength went up practically only in the two last steps of stabilization and finishing. The ultimate strain, relatively high in the unoriented less crystalline TF, decreased about six times during the biorientation and further on, decreased in the last two steps; this could have been due to an increase of local defects.

Permeability to Gases

Nylon 6 is known to be a moderately good barrier material to O_2 and N_2 in dry conditions. Table VII shows the values of permeability to O_2, N_2, and CO_2 both for the BF and for the stabilized STs. Permeability decreased in the order $CO_2 > O_2 > N_2$. For all the films, permeability values did not change significantly after the stretching and stabilization treatments; because of the very low permeability values, near to the sensitivity limit of the equipment, permeability differences due to thermomechanical treatments were in the range of the experimental errors. In conclusion, the biorientation step or other thermomechanical treatments did not influence significantly the absolute value of permeability.

CONCLUSIONS

The physicochemical properties of nylon 6 films were analyzed during the various steps of the technological production continuous process, from the extruded TF to a thin film for packaging use. Manufacture brings a reduction in the film thickness, of about 10 times, and significantly improves the mechanical properties of the product, such as elastic modulus, σ_y, and strength and decreases the film deformability. The TF is made up of about 40% crystalline phase, a mainly unstable γ phase formed during the quenching in water, and 60% amorphous phase. The blowing step has a double effect on nylon structure: it transforms the unstable γ phase into the more stable α phase and increases crystallinity with a decrease of the amorphous phase. Indeed, the blowing step is responsible for the thickness reduction and for a biaxial orientation. The stabilization step increases further the α phase with a decrease in amorphous phase as shown by X-rays and IR analysis.

Elastic modulus increases because of blowing and appreciably after the stabilization and the final step. The strong variation in the mechanical properties can be

TABLE VII
Gas Permeability[a] of Some Dry Gases

Film type	Oxygen	Nitrogen	Carbon dioxide
BF	1.	0.2	3
ST	0.5	0.1	2

[a] $[(\text{STP cm}^3)/(\text{cm}^2 \cdot \text{s} \cdot \text{cmHg})] \times 10^{12}$.

explained by the assumption that during the biorientation stretching, polymer chains in the amorphous phase rearrange with the formation of more hydrogen bonds between themselves and with the crystalline domains.

The permeability of various films, on the contrary, are not significantly influenced by the process steps, notwithstanding the increase in crystallinity and the orientation of macromolecular chains due to stretching and stabilization. This can be justified on the basis of a very small variation of the free volume, as shown by PAS, which evidenced no variation of the mean hole volume and a small variation of hole number during the different steps. PAS analysis suggested that a very small variation in the diffusion coefficient may be expected. The gas solubility of the polymer has to be independent from the thermomechanical treatments, which mainly cause changes in orientation of the crystallinity domains but do not change the chemical nature of the gas sorption centers. Because no appreciable variation in the hole volume responsible for the diffusion coefficient was found, no change in the gas permeability is to be expected.

References

1. Perone, C. Poliplasti 1985, 347, 60.
2. Kohan, M. I. Nylon Plastics Handbook; Munich: Hanser, 1995; p 120.
3. McCrumm, N. G.; Buchley, C. P.; Buchnall, C. B. Principles of Polymer Engineering; Oxford: Oxford University Press, 1995; p 164.
4. Kansy, J. Nucl Instrum Methods A 1996, 374, 235.
5. Zanderighi, L.; Bianchi, F.; Monga, R.; Pegoraro, M. Chim Ind Milan 1990, 72, 147.
6. Huisman, R.; Heuvel, H. M. J Polym Sci 1976, 14, 921.
7. Huisman, R.; Heuvel, H. M. J Polym Sci 1976, 14, 941.
8. Roldan, L. C.; Kaufman, H. S. J Polym Sci Polym Lett Ed 1963, 1, 603.
9. Arimoto, H.; Ishibashi, M.; Hirai, M.; Chatani, Y. J Polym Sci 1965, 3, 317.
10. Schneider, B.; Sebraidt, P.; Wichterle, O. Collect Czech Chem Commun 1962, 27, 1749.
11. Doskocilova, D.; Picova, H.; Schneider, B.; Cefelin, P. Collect Czech Chem Commun 1963, 28, 1867.
12. Sanderman, I.; Keller, A. J Polym Sci 1956, 19, 401.
13. Jake, J.; Schmidt, P.; Schneider, B. Collect Czech Chem Commun 1965, 30, 996.
14. Tao, S. J. J Chem Phys 1972, 56, 5499.
15. Eldrup, M.; Lightbody, D.; Sherwood, N. J Chem Phys 1981, 63, 51.
16. Dupasquier, A.; DeNatale, P.; Rolando, A. Phys Rev B 1991, 43, 10036.
17. Nakanishi, H.; Ujihira, Y. J. J Phys Chem 1982, 86, 4446.
18. Gregory, R. B. J Appl Phys 1991, 70, 4665.
19. Jean, Y. C. In Positron and Positronium Chemistry; Jean, Y. C., Ed.; World Scientific: Singapore, 1990; p 1.